Crystal structure of the human symplekin-Ssu72-CTD phosphopeptide complex

Kehui Xiang[1], **Takashi Nagaike**[1,*], **Song Xiang**[1,2,*], **Turgay Kilic**[1], **Maia M. Beh**[1], **James L. Manley**[1], and **Liang Tong**[1]

[1] Department of Biological Sciences, Columbia University, New York, NY 10027, USA

Abstract

Symplekin (Pta1 in yeast) is a scaffold in the large protein complex that is required for 3′-end cleavage and polyadenylation of eukaryotic messenger RNA precursors (pre-mRNAs) [1–4], and also participates in transcription initiation and termination by RNA polymerase II (Pol II) [5,6]. Symplekin mediates interactions among many different proteins in this machinery [1,2,7–9], although the molecular basis for its function is not known. Here we report the crystal structure at 2.4 Å resolution of the N-terminal domain (residues 30–340) of human symplekin (Symp-N) in a ternary complex with the Pol II C-terminal domain (CTD) Ser^5 phosphatase Ssu72 [7,10–17] and a CTD Ser^5 phosphopeptide. The N-terminal domain of symplekin has the ARM or HEAT fold, with seven pairs of anti-parallel α-helices arranged in the shape of an arc. The structure of Ssu72 has some similarity to that of low-molecular-weight phosphotyrosine protein phosphatase [18,19], although Ssu72 has a unique active site landscape as well as extra structural features at the C-terminus that is important for interaction with symplekin. Ssu72 is bound to the concave face of symplekin, and engineered mutations in this interface can abolish interactions between the two proteins. The CTD peptide is bound in the active site of Ssu72, unexpectedly with the pSer^5-Pro^6 peptide bond in the *cis* configuration, which contrasts with all other known CTD peptide conformations [20,21]. While the active site of Ssu72 is about 25 Å away from the interface with symplekin, we found that the symplekin N-terminal domain stimulates Ssu72 CTD phosphatase activity *in vitro*. Furthermore, the N-terminal domain of symplekin inhibits polyadenylation *in vitro*, but importantly only when coupled to transcription. As catalytically active Ssu72 overcomes this inhibition, our results demonstrate a role for mammalian Ssu72 in transcription-coupled pre-mRNA 3′-end processing.

Keywords

pre-mRNA processing; protein complex; protein phosphatase; RNA polymerase II; transcription; peptidyl-prolyl isomerase

Human symplekin contains 1274 amino acid residues (Fig. 1a) and its sequence is well conserved among higher eukaryotes (Supplementary Fig. 1). In comparison, symplekin shares only weak sequence similarity with yeast Pta1 [1] (Supplementary Fig. 2), and Pta1 lacks the C-terminal 500 residues of symplekin (Fig. 1a). Symplekin and Pta1 do not have any recognizable homology with other proteins. Secondary-structure predictions suggest the presence of an all-helical segment in the N-terminal region of symplekin and Pta1 (Fig. 1a and Supplementary Figs. 1–2). Recent studies in yeast suggested that the N-terminal segment of Pta1 is important for interaction with Ssu72 [9]. Ssu72 is required for pre-mRNA 3′-end cleavage in yeast [7], although its phosphatase activity is not necessary for this function [13]. The catalytic activity of Ssu72 may instead be important for Pol II transcription and termination, and gene looping [17]. Ssu72 is highly conserved among the eukaryotes (Supplementary Fig. 3), but to date no evidence exists implicating mammalian Ssu72 in 3′-end processing.

To determine the structure of a symplekin-Ssu72-CTD phosphopeptide ternary complex, residues 30–360 of human symplekin and full-length human Ssu72 were over-expressed and purified separately. The two proteins were mixed, with Ssu72 in slight molar excess, and the symplekin-Ssu72 complex was purified by gel-filtration chromatography. This procedure also demonstrated strong interactions between the two human proteins, consistent with observations on their yeast counterparts [9]. The 10-mer CTD phosphopeptide used in this study, $SY^1S^2P^3T^4(pS^5)P^6S^7YS$, where Ser^5 is phosphorylated, contained an entire CTD heptad repeat as well as a Ser from the previous repeat and Tyr-Ser from the following repeat. To prevent hydrolysis, the active site nucleophile Cys12 of Ssu72 was mutated to Ser in the ternary complex. We have also determined the crystal structure of the symplekin-Ssu72(wild-type) binary complex and the structures of the symplekin N-terminal domain alone (for residues 30–395, 30–360, or 1–395). All the structures have excellent agreement with the crystallographic data and the expected geometric parameters (Supplementary Table 1).

The structures show that residues 30–340 of symplekin (Symp-N) form seven pairs of anti-parallel α-helices, while residues 1–29 and 341–395 are disordered (Supplementary Fig. 1). The pairs of helices are arranged in the shape of an arc, with the first helix in each pair, the αA helix, being located on the convex face of the arc, and the αB helix on the concave face (Fig. 1b). Most of the loops connecting the helices are short, except for that linking helices α4B and α5A, with 31 residues (Fig. 1b). The overall fold of Symp-N is found in many other proteins, including those with the ARM or HEAT repeats. These structures are often involved in protein-protein interactions, consistent with the proposed scaffold function of symplekin.

The structure of the N-terminal domain of *Drosophila* symplekin (residues 22–270) was reported recently [22]. Its overall conformation is similar to that of human Symp-N, with rms

distance of 1.0 Å among their equivalent Cα atoms, although the *Drosophila* symplekin structure is missing the two pairs of helices (α6 and α7) at the C-terminus (Fig. 1c). Noting the good sequence conservation of residues in this region (Supplementary Fig. 1), it is likely that these helices are also present in the N-terminal domain of *Drosophila* symplekin. Notably, our studies show that helix α6B is important for interactions with Ssu72 (Fig. 1b, see below).

The structure of Ssu72 contains a central 5-stranded β-sheet (β1 through β5) that is surrounded by helices on both sides (Fig. 2a, Supplementary Fig. 4). The closest structural homolog of Ssu72 is the low-molecular-weight phosphotyrosine protein phosphatase (Fig. 2b) [18],[19], as suggested earlier [11],[12],[14], even though the two proteins share only 16% sequence identity. Our studies show however that Ssu72 possesses three unique structural features as compared to this other phosphatase (Fig. 2b), which are formed by highly conserved residues (Supplementary Fig. 3) and have important functions. A small, two-stranded anti-parallel β-sheet (β2A and β2B) is located near the active site (Fig. 2a). The αD helix is in a different conformation in Ssu72 and also contributes to phosphopeptide binding. Finally, Ssu72 contains an extra helix (αG) andβ-strand (β5) at the C-terminus, which are essential for interactions with symplekin (Fig. 1b).

Our structure of the ternary complex showed that the CTD phosphopeptide, with good electron density for residues Thr[4] to Ser[7] (Fig. 2c), is bound with the peptide bond between pSer[5] and Pro[6] in the *cis* configuration (Fig. 2d). This is in sharp contrast to the conformations of the CTD phosphopeptides observed in other structures, which all have the Pro residue(s) in the *trans* configuration (Supplementary Fig. 5) [20],[21]. With the *cis* configuration, the backbone of the phosphopeptide makes a 180° turn at the pSer-Pro residues, while the peptide in the *trans* configuration (Supplementary Fig. 5) would clash with Ssu72. Therefore, Ssu72 can only bind and dephosphorylate CTD substrates with the pSer-Pro peptide bond in the *cis* configuration, in contrast to all other known CTD phosphatases (Supplementary text).

Our observation of a *cis* configuration for the CTD also provides a different interpretation for the role of the peptidyl-prolyl isomerase Pin1 (Ess1 in yeast) in regulating Pol II transcription [23]–[25]. It has been proposed that Pin1/Ess1 promotes the *trans* configuration of the CTD for dephosphorylation by Ssu72 [24],[25], while our structure indicates that the opposite must be true. Our *in vitro* phosphatase assays demonstrate that Pin1 strongly stimulates the phosphatase activity of Ssu72 (Supplementary text and Supplementary Fig. 6), consistent with its specificity for the *cis* configuration.

The active site of Ssu72 is located at the bottom of a narrow groove (Fig. 2e), one wall of which is formed by the small β-sheet (β2A and β2B) and the loop linking the two strands (Fig. 2d). This severely limits the possible conformation of the CTD, ensuring that only the *cis* configuration of the pSer-Pro peptide bond can be accommodated in the active site. In fact, the Thr[4]-pSer[5] peptide bond is π-stacked with the Pro[6]-Ser[7] peptide bond (Fig. 2d), suggesting a highly restrained conformation for the CTD phosphopeptide in this region. Residues Thr[4], pSer[5] and Pro[6] of the same repeat as well as Tyr[1] of the following repeat have interactions with the enzyme (Supplementary text, Fig. 2d), explaining the preference

for pSer[5] by Ssu72 and consistent with results from earlier biochemical studies on yeast Ssu72 [14].

The phosphate group of the peptide is bound deepest in the structure, having extensive ion-pair and hydrogen-bonding interactions with the enzyme (Fig. 2d). In addition, the main-chain amide group of pSer[5] is hydrogen-bonded to the main-chain carbonyl of Lys43 (in β2A). The catalytic nucleophile of Ssu72, Cys12, is located directly below the phosphate group and can be in the correct position for the inline nucleophilic attack on the phosphorus atom to initiate the reaction (Supplementary Fig. 7). The side chain of Asp143 is located 3.5 Å from the Oγ atom of Ser[5], consistent with its role as the general acid to protonate the leaving group. There are some conformational changes in the active site region of Ssu72, especially for the β2A-β2B loop, upon binding of the CTD phosphopeptide (Supplementary Fig. 7), although this loop appears to be flexible and can assume different conformations in the various structures.

In the structures of the binary and ternary complexes, Ssu72 is bound to the concave face of the Symp-N (Fig. 1b). Approximately 950 Å^2 of the surface area of each protein is buried in the interface of this complex, which involves helices α3B through α6B of Symp-N (Fig. 3a, Supplementary Fig. 1), and helix αE, the followingαE-β4 loop, helix αG and strand β5 of Ssu72 (Supplementary Fig. 3). In addition, residue Arg206, at the tip of the long loop connecting helices α4B and α5A of Symp-N, is also located in the interface (Fig. 3a). Ion-pair, hydrogen-bonding as well as hydrophobic interactions make contributions to the formation of this complex (Supplementary text). Especially, the side chains of Val191 and Phe193 of Ssu72 (in strand β5) establish hydrophobic interactions with those of Lys185 (α4B) and Ile251 (α5B) of symplekin in the center of this interface (Fig. 3a). In addition, the side chain hydroxyl group of Thr190 (β5) of Ssu72 is hydrogen-bonded to the side chain of Asn300 (α6B) of symplekin. The relative positions of Symp-N and Ssu72 appear to be somewhat variable among the binary and ternary complexes (Supplementary text, Supplementary Fig. 8).

The symplekin-Ssu72 interface is located about 25 Å from the active site of Ssu72 (Fig. 1b). Unexpectedly however, phosphatase assays measuring hydrolysis of a *p*-nitrophenylphosphate (pNPP) model substrate [11],[12] showed that Symp-N stimulated Ssu72 activity (Fig. 3b), and maximal activation was achieved when the two proteins were at 1:1 molar ratio. To assess whether this stimulation also occurs with a natural substrate, we first used the 10-mer CTD phosphopeptide in the assay, monitoring the release of inorganic phosphate, and observed a similar stimulation (Supplementary Fig. 6). We next prepared a GST-CTD fusion protein that had been phosphorylated on Ser[2] and Ser[5] with HeLa nuclear extract [26]. As demonstrated by Western blotting with a pSer[5] specific antibody, Ssu72 dephosphorylated this protein on Ser[5], importantly in a manner that was also stimulated by Symp-N (Fig. 3c). Ssu72 was specific for dephosphorylating pSer[5], as Ser[2] phosphorylation, as monitored by a pSer[2] specific antibody, was not affected (data not shown).

Our data indicate that the symplekin-Ssu72 interaction activated Ssu72 phosphatase activity, likely through stabilization of the Ssu72 structure and/or an allosteric mechanism. This is consistent with previous studies on the R129A mutant (*ssu72-2*) of yeast Ssu72, equivalent

to Arg126 in human Ssu72 (Supplementary Fig. 3). This mutant displays a two-fold reduction in catalytic activity compared to wild-type Ssu72 and produces a severe growth defect at the non-permissive temperature [16]. Arg126 is far from the active site and is in fact near the interface with symplekin (Fig. 3a). However, it does not directly contribute to interactions with symplekin, and the R126A mutation did not disrupt interaction with Symp-N (data not shown).

To assess the importance of individual residues for the stability of the symplekin-Ssu72 complex, we introduced mutations in the interface and characterized their effects on the complex using gel-filtration chromatography and phosphatase assays. The presence of wild-type Ssu72 gave rise to a clear shift of the peak for Symp-N from a gel-filtration column (Fig. 3d), corresponding to the formation of the symplekin-Ssu72 complex. Ssu72 was present in two-fold molar excess in this experiment, and only half of this protein was incorporated into the complex (Fig. 3d), demonstrating a 1:1 stoichiometry for the complex. Mutation of a symplekin residue in the interface, K185A (Fig. 3a), essentially abolished the interaction with wild-type Ssu72 (Fig. 3e), and mutation of three Ssu72 residues in the interface, T190A/V191A/F193A, abolished the interaction with wild-type symplekin. The chromatographic behavior of the mutants alone was similar to that of the wild-type protein (Fig. 3e), suggesting that the mutations did not disrupt the structure of the proteins. This was also confirmed by the crystal structure of the K185A mutant (data not shown). Consistent with the gel-filtration data, the symplekin K185A mutant failed to stimulate Ssu72 phosphatase activity, and the T190A/V191A/F193A mutant of Ssu72 could not be stimulated by wild-type Symp-N (Fig. 3b).

We next wished to assess the functional importance of the symplekin-Ssu72 interaction with respect to 3′-end formation. Given the roles of their yeast counterparts in both transcription and polyadenylation, we used a transcription-coupled 3′-end processing assay [27]. HeLa nuclear extract was pre-incubated with increasing concentrations of Symp-N, which led to a pronounced inhibition of polyadenylation (Fig. 4a), similar to an effect observed earlier with the yeast Pta1 N-terminal domain in a transcription-independent assay [9]. Transcription, as measured by accumulation of unprocessed pre-mRNA, was not affected (Fig. 4b). Unexpectedly, RNase protection assays showed that 3′-end cleavage was also not affected (Supplementary Fig. 9), indicating that Symp-N affects only the polyadenylation step of 3′-end formation. Inclusion of purified Ssu72 during the pre-incubation with Symp-N blocked the inhibition, while Ssu72 alone had no effect (Fig. 4c). Importantly, the K185A mutation in Symp-N abolished this inhibitory effect, while the T190A/V191A/F193A mutant of Ssu72 failed to overcome the inhibition by wild-type Symp-N (Fig. 4c). These results provide strong evidence that the inhibitory effect of Symp-N reflects its interaction with Ssu72, and thus implicates Ssu72 in mammalian 3′-end processing. Somewhat unexpectedly, based on studies in yeast [7,9], the catalytically inactive C12S mutant of Ssu72 failed to overcome this inhibition (Fig. 4c), and Symp-N had no detectable effect on transcription-independent polyadenylation (Fig. 4d and data not shown). Together, these results indicate that Ssu72 phosphatase activity is required for polyadenylation of pre-mRNAs, but only when processing is coupled to transcription.

Our finding that a CTD phosphopeptide is bound to Ssu72 with the pSer-Pro peptide bond in the *cis* configuration indicates the existence of a novel CTD conformation. While Ssu72 has been well studied in yeast and has functions in transcription and 3′-end processing, essentially nothing was known about its mammalian counterpart. In fact, while the yeast enzyme is a stable component of the polyadenylation machinery and required for processing, mammalian Ssu72 has not been found associated with polyadenylation factors, and was not detected in a recent proteomic analysis of the assembled polyadenylation complex [28]. Consistent with this, our results provide evidence that in mammals Ssu72 is only necessary for polyadenylation when processing is coupled to transcription. A parsimonious model is that symplekin recruits Ssu72 to the transcription complex and activates its phosphatase activity, which promotes polyadenylation. Conceivably this occurs by facilitating recruitment of poly(A) polymerase, known for many years to be only weakly associated with other 3′-end processing factors [28],[29], to the complex. Given that the CTD is necessary for efficient 3′-end formation in mammalian cells [26],[30], and that CTD pSer[5] is the only known target of Ssu72, CTD pSer[5] dephosphorylation may well be important in facilitating polyadenylation during transcription.

Methods summary

Crystallography

The N-terminal domain of human symplekin and full-length human Ssu72 were over-expressed separately in *E. coli* and purified. The symplekin-Ssu72 complex was purified by gel filtration of a mixture of the two proteins. Crystals were obtained by the sitting-drop vapor diffusion method, and the structures were determined by the seleno-methionyl single-wavelength anomalous diffraction method and the molecular replacement method.

In vitro transcription-coupled polyadenylation assay

Transcription-coupled polyadenylation was carried out using a DNA construct containing GAL4 binding sites upstream of the adenovirus E4 core promoter and SV40 late poly(A) site downstream. Recombinant symplekin and Ssu72 proteins were preincubated with HeLa nuclear extract before transcription was started by adding the DNA template and purified GAL4-VP16. RNA products were purified, separated into nonpolyadenylated and polyadenylated fractions and analyzed on 5% denaturing gel. Radioactivity was detected using a Phosphorimager. Assays were repeated multiple times with consistent results.

Full Methods and any associated references are available in the online version of the paper at www.nature.com/nature.

Supplementary Material

Refer to Web version on PubMed Central for supplementary material.

Acknowledgments

References

1. Takagaki Y, Manley JL. Complex protein interactions within the human polyadenylation machinery identify a novel component. Mol Cell Biol. 2000; 20:1515–1525. [PubMed: 10669729]

2. Zhao J, Kessler MM, Helmling S, O'Connor JP, Moore CL. Pta1, a component of yeast CFII, is required for both cleavage and poly(A) addition of mRNA precursor. Mol Cell Biol. 1999; 19:7733–7740. [PubMed: 10523662]

3. Zhao J, Hyman L, Moore CL. Formation of mRNA 3′ ends in eukaryotes: mechanism, regulation, and interrelationships with other steps in mRNA synthesis. Microbiol Mol Biol Rev. 1999; 63:405–445. [PubMed: 10357856]

4. Mandel CR, Bai Y, Tong L. Protein factors in pre-mRNA 3′-end processing. Cell Mol Life Sci. 2008; 65:1099–1122. [PubMed: 18158581]

5. Calvo O, Manley JL. Strange bedfellows: polyadenylation factors at the promoter. Genes Develop. 2003; 17:1321–1327. [PubMed: 12782649]

6. Moore MJ, Proudfoot NJ. Pre-mRNA processing reaches back to transcription and ahead to translation. Cell. 2009; 136:688–700. [PubMed: 19239889]

7. He X, et al. Functional interactions between the transcription and mRNA 3′ end processing machineries mediated by Ssu72 and Sub1. Genes Develop. 2003; 17:1030–1042. [PubMed: 12704082]

8. Nedea E, et al. Organization and function of APT, a subcomplex of the yeast cleavage and polyadenylation factor involved in the formation of mRNA and small nucleolar RNA 3′-ends. J Biol Chem. 2003; 278:33000–33010. [PubMed: 12819204]

9. Ghazy MA, He X, Singh BN, Hampsey M, Moore C. The essential N terminus of the Pta1 scaffold protein is required for snoRNA transcription termination and Ssu72 function but is dispensible for pre-mRNA 3′-end processing. Mol Cell Biol. 2009; 29:2296–2307. [PubMed: 19188448]

10. Dichtl B, et al. A role for SSU72 in balancing RNA polymerase II transcription elongation and termination. Mol Cell. 2002; 10:1139–1150. [PubMed: 12453421]

11. Meinhart A, Silberzahn T, Cramer P. The mRNA transcription/processing factor Ssu72 is a potential tyrosine phosphatase. J Biol Chem. 2003; 278:15917–15921. [PubMed: 12606538]

12. Ganem C, et al. Ssu72 is a phosphatase essential for transcription termination of snoRNAs and specific mRNAs in yeast. EMBO J. 2003; 22:1588–1598. [PubMed: 12660165]

13. Krishnamurthy S, He X, Reyes-Reyes M, Moore CL, Hampsey M. Ssu72 is an RNA polymerase II CTD phosphatase. Mol Cell. 2004; 14:387–394. [PubMed: 15125841]

14. Hausmann S, Koiwa H, Krishnamurthy S, Hampsey M, Shuman S. Different strategies for carboxyl-terminal domain (CTD) recognition by serine 5-specific CTD phosphatases. J Biol Chem. 2005; 280:37681–37688. [PubMed: 16148005]

15. St-Pierre B, et al. Conserved and specific functions of mammalian ssu72. Nucl Acid Res. 2005; 33:464–477.

16. Reyes-Reyes M, Hampsey M. Role for the Ssu72 C-terminal domain phosphatase in RNA polymerase II transcription elongation. Mol Cell Biol. 2007; 27:926–936. [PubMed: 17101794]

17. Ansari A, Hampsey M. A role for the CPF 3′-end processing machinery in RNAP II-dependent gene looping. Genes Develop. 2005; 19:2969–2978. [PubMed: 16319194]

18. Su XD, Taddei N, Stefani M, Ramponi G, Nordlund P. The crystal structure of a low-molecular-weight phosphotyrosine protein phosphatase. Nature. 1994; 370:575–578. [PubMed: 8052313]

19. Zhang M, Van Etten RL, Stauffacher CV. Crystal structure of bovine heart phosphotyrosyl phosphatase at 2.2-Å resolution. Biochem. 1994; 33:11097–11105. [PubMed: 7537084]

20. Meinhart A, Kamenski T, Hoeppner S, Baumli S, Cramer P. A structural perspective of CTD function. Genes Develop. 2005; 19:1401–1415. [PubMed: 15964991]

21. Zhang Y, et al. Determinants for dephosphorylation of the RNA polymerase II C-terminal domain by Scp1. Mol Cell. 2006; 24:759–770. [PubMed: 17157258]

22. Kennedy SA, et al. Crystal structure of the HEAT domain from the pre-mRNA processing factor symplekin. J Mol Biol. 2009; 392:115–128. [PubMed: 19576221]

23. Xu YX, Hirose Y, Zhou XZ, Lu KP, Manley JL. Pin1 modulates the structure and function of human RNA polymerase II. Genes Develop. 2003; 17:2765–2776. [PubMed: 14600023]

24. Krishnamurthy S, Ghazy MA, Moore C, Hampsey M. Functional interaction of the Ess1 prolyl isomerase with components of the RNA polymerase II initiation and termination machineries. Mol Cell Biol. 2009; 29:2925–2934. [PubMed: 19332564]

25. Singh N, et al. The Ess1 prolyl isomerase is required for transcription termination of small noncoding RNAs via the Nrd1 pathway. Mol Cell. 2009; 36:255–266. [PubMed: 19854134]

26. Hirose Y, Manley JL. RNA polymerase II is an essential mRNA polyadenylation factor. Nature. 1998; 395:93–96. [PubMed: 9738505]

27. Rozenblatt-Rosen O, et al. The tumor suppressor Cdc73 functionally associates with CPSF and CstF 3′ mRNA processing factors. Proc Natl Acad Sci USA. 2009; 106:755–760. [PubMed: 19136632]

28. Shi Y, et al. Molecular architecture of the human pre-mRNA 3′ processing complex. Mol Cell. 2009; 33:365–376. [PubMed: 19217410]

29. Takagaki Y, Ryner LC, Manley JL. Separation and characterization of a Poly(A) polymerase and a cleavage/specificity factor required for pre-mRNA polyadenylation. Cell. 1988; 52:731–742. [PubMed: 2830992]

30. McCracken S, et al. The C-terminal domain of RNA polymerase II couples mRNA processing to transcription. Nature. 1997; 385:357–361. [PubMed: 9002523]
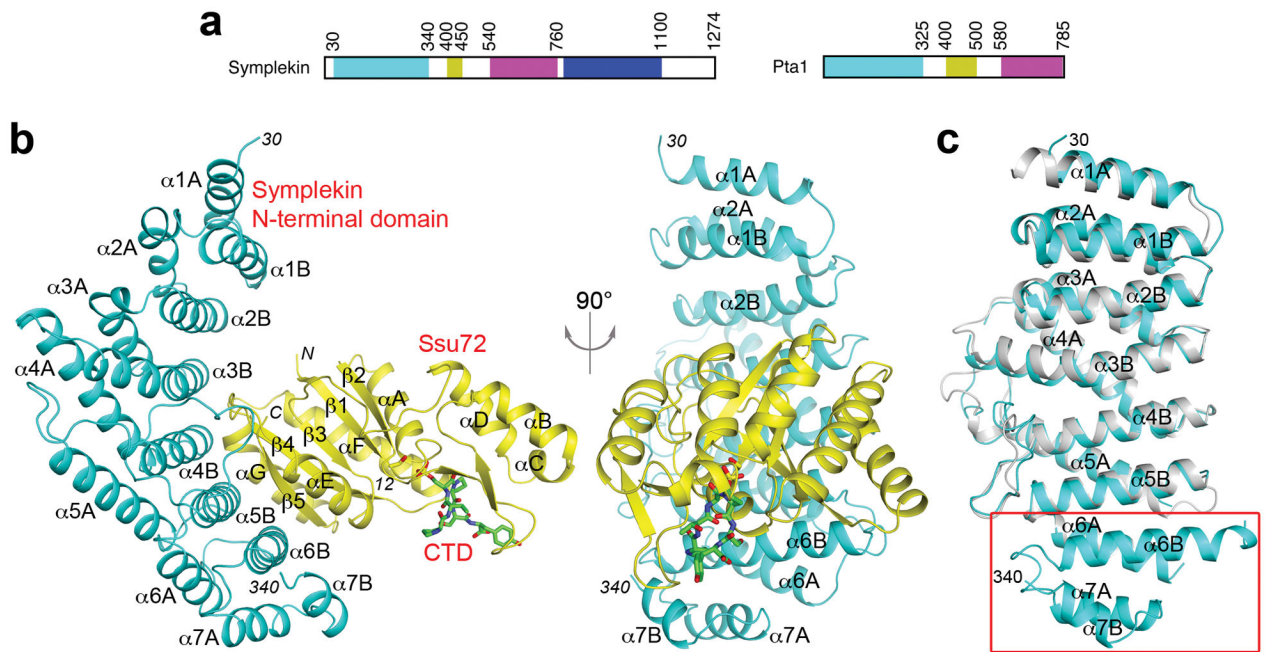
Figure 1. Structure of the human symplekin-Ssu72-CTD phosphopeptide ternary complex
(**a**). Domain organization of human symplekin and *S. cerevisiae* Pta1. The domains are
suggested by secondary structure predictions, and the middle region of Pta1 is suggested by
functional studies [9]. (**b**). Schematic drawing of the structure of human symplekin-Ssu72-
CTD phosphopeptide ternary complex, in two views. The N-terminal domain of symplekin
is shown in cyan, and Ssu72 in yellow. The CTD phosphopeptide is shown as a stick model
(in green for carbon atoms). (**c**). Overlay of the structures of the N-terminal domain of
human (in cyan) and *Drosophila* (in gray) symplekin [22]. *Drosophila* symplekin is missing
the last two pairs of helical repeats (boxed). All structure figures were produced with
PyMOL (www.pymol.org).
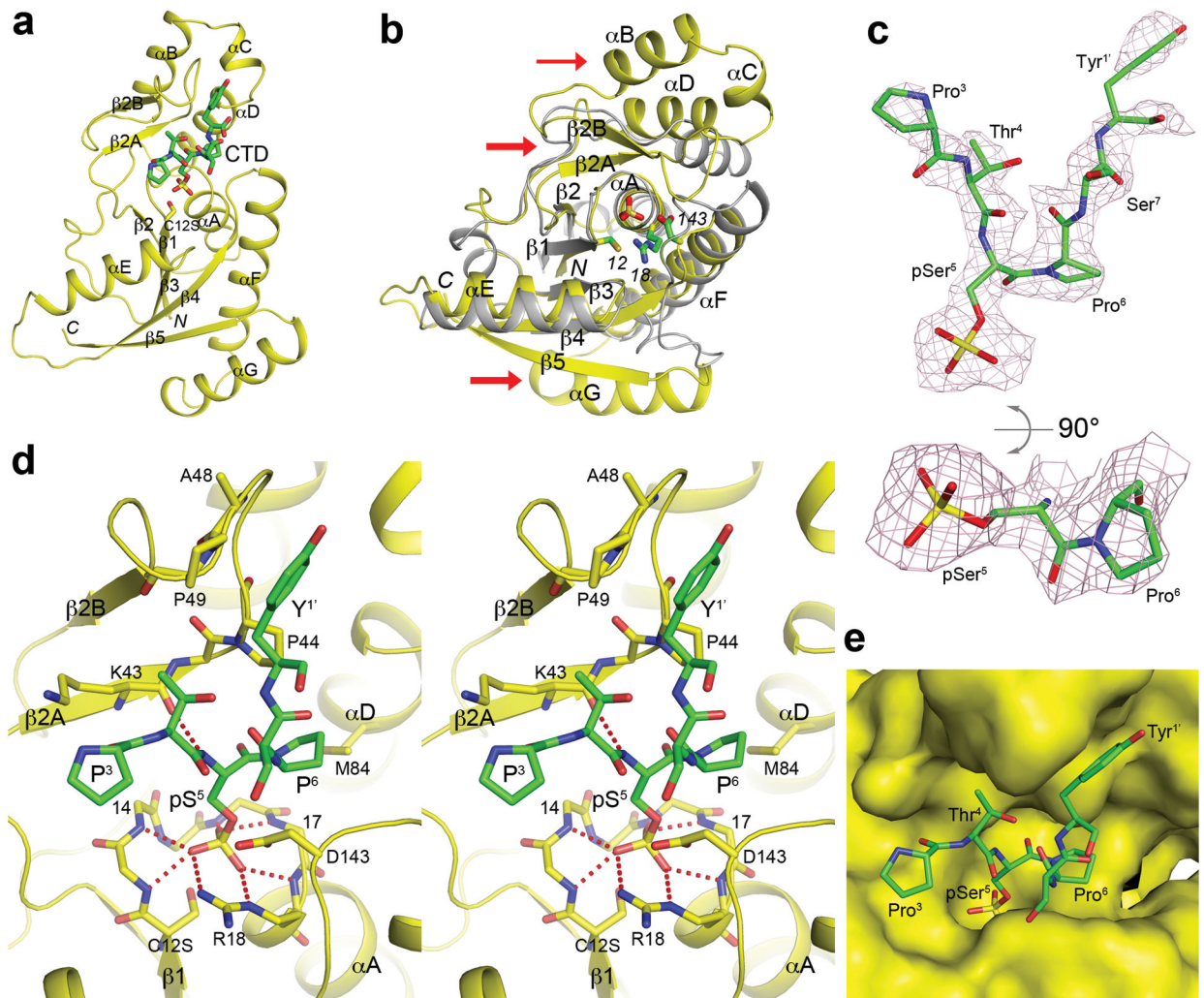
Figure 2. Recognition of the CTD phosphopeptide by human Ssu72

(**a**). Schematic drawing of the structure of human Ssu72-CTD phosphopeptide complex. (**b**). Overlay of the structures of Ssu72 (yellow) and low-molecular-weight phosphotyrosine protein phosphatase (gray) [18],[19]. Arrows point to unique structural features in Ssu72. For stereo version of **a** and **b**, please see Supplementary Fig. 4. (**c**). Two views of the omit F_o–F_c electron density at 2.4 Å resolution for the CTD phosphopeptide, contoured at 3σ. (**d**). Detailed interactions between the CTD phosphopeptide and the active site of Ssu72. Ion-pair and hydrogen-bonding interactions are indicated with the dashed lines in red. (**e**). Molecular surface of the active site region of Ssu72. The CTD phosphopeptide is shown as a stick model.
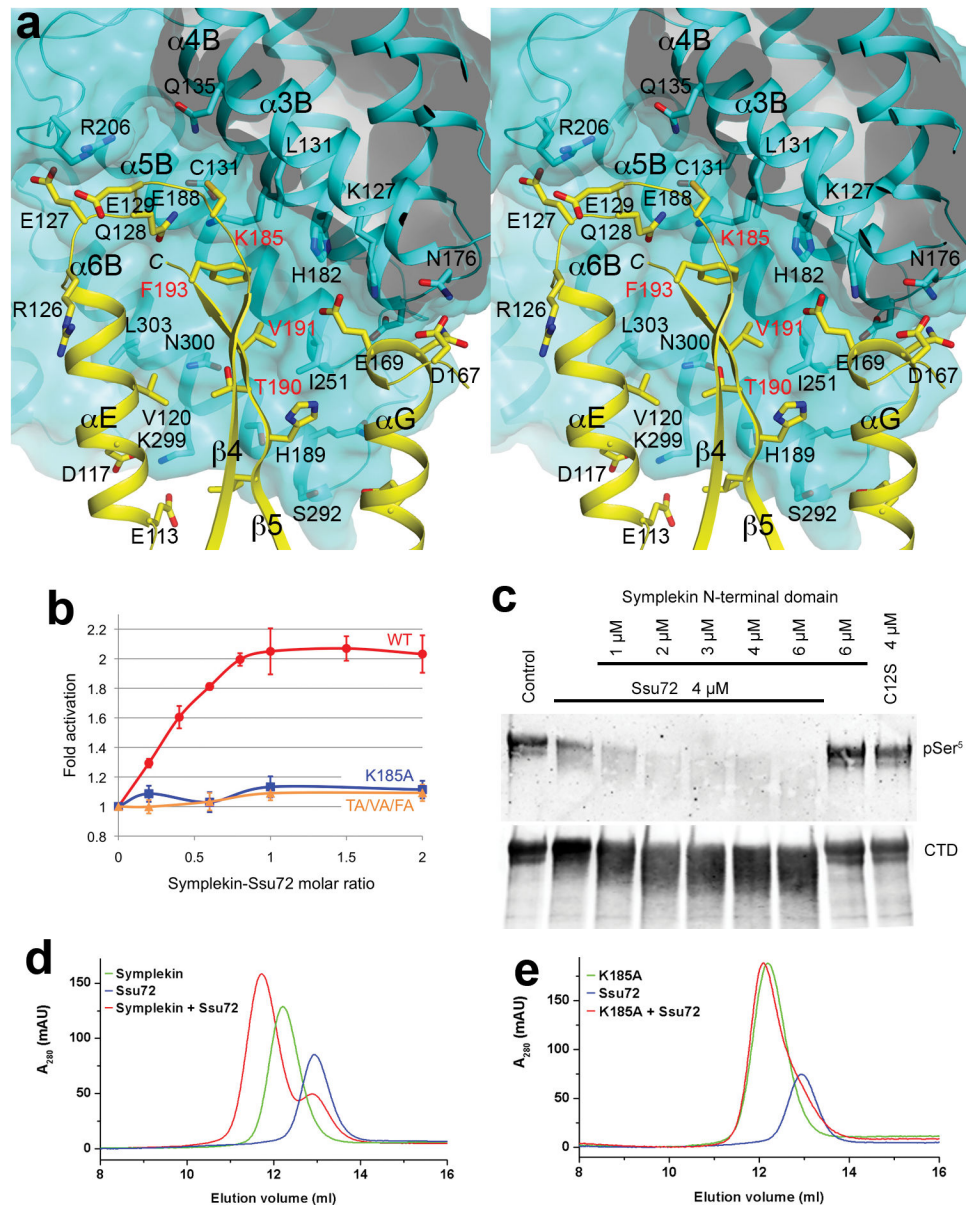
Figure 3. Structural and biochemical characterizations of the symplekin-Ssu72 interface
(**a**). Detailed interactions between symplekin (in cyan) and Ssu72 (in yellow) in the interface. The molecular surface of symplekin is also shown (in cyan). Side chains making important contributions to the interface are shown as stick models. Residues labeled in red were selected for mutagenesis. (**b**). The activity of Ssu72, measured by the hydrolysis of pNPP, as a function of the molar ratio of symplekin is shown. TA/VA/FA: T190A/V191A/F193A mutant of Ssu72 (stimulation by wild-type symplekin). The error bars are ±SD, from three independent experiments. (**c**). Stimulation of the CTD Ser^5 phosphatase activity of Ssu72 by symplekin. The levels of pSer^5 and total CTD were determined using the H14 and 8WG16 antibodies, respectively. (**d**). Gel-filtration profiles for wild-type symplekin N-terminal domain alone, wild-type human Ssu72 (full-length) alone, and their mixture (with
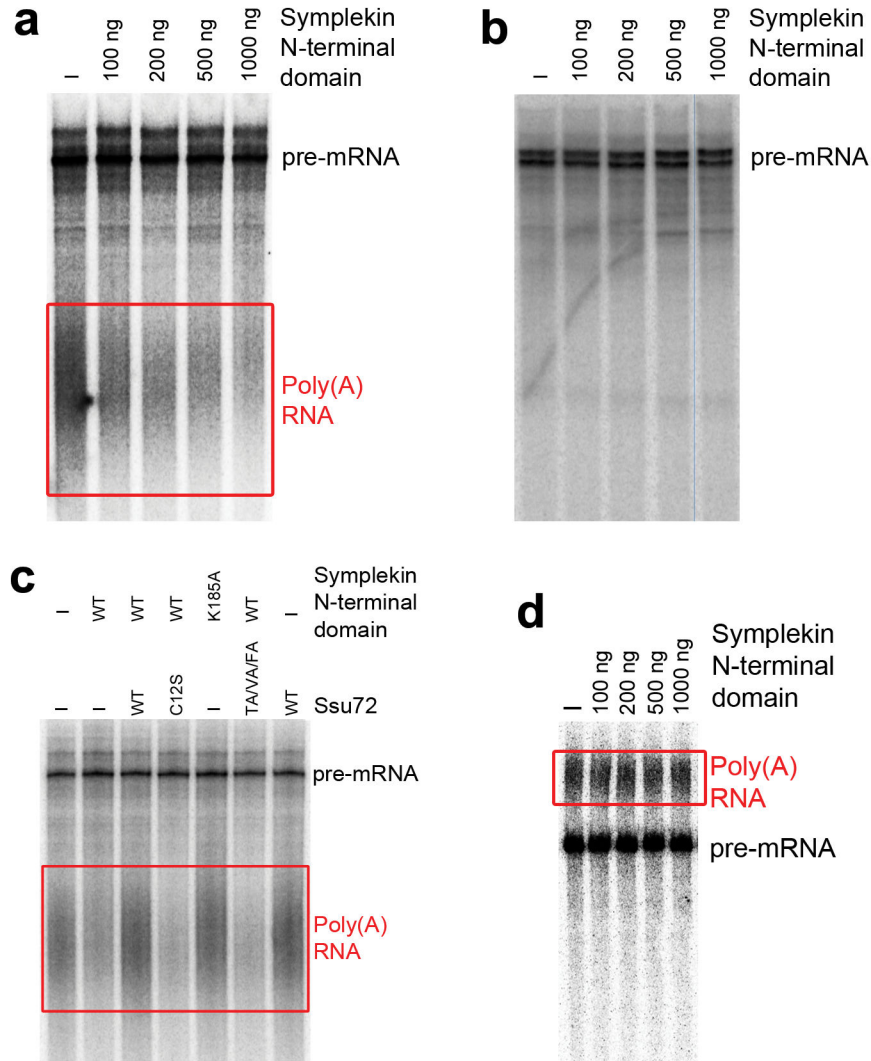
Ssu72 present in roughly 2-fold molar excess). (**e**). Gel-filtration profiles for wild-type Ssu72 alone, K185A mutant of symplekin alone, and their mixture.

Figure 4. Functional characterization of the symplekin-Ssu72 interaction

(**a**). Transcription-coupled polyadenylation is inhibited in a dose-dependent fashion by symplekin N-terminal domain. Transcription-processing was performed in HeLa nuclear extract, RNAs purified and separated into poly(A)-and poly(A)+ fractions, and resolved by denaturing PAGE. Positions of unprocessed "run-off" RNA (pre-mRNA) and cleaved and polyadenylated RNA (poly(A) RNA) are indicated. (**b**). Symplekin N-terminal domain does not inhibit transcription. Poly(A)- RNAs (2%) from the transcription-coupled polyadenylation assays in the presence of increasing concentrations of symplekin N-terminal domain are shown. (**c**). Ssu72 overcomes the inhibition of transcription-coupled polyadenylation by symplekin. The effects of the K185A mutant of symplekin and the C12S and T190A/V191A/F193A (labeled TA/VA/FA) mutants of Ssu72 on polyadenylation are also shown. (**d**). Polyadenylation of SV40 late pre-mRNA, uncoupled to transcription, is not inhibited by symplekin N-terminal domain.